Journal of Materials Processing Tech. 282 (2020) 116684

Contents lists available at ScienceDirect

Journal of Materials Processing Tech.

journal homepage: www.elsevier.com/locate/jmatprotec

On the mechanical integrity of AA6082 3D structures deposited by hybrid metal extrusion & bonding additive manufacturing

Jørgen Blindheim[a,*], Øystein Grong[a,b], Torgeir Welo[a], Martin Steinert[a]

[a] Norwegian University of Science and Technology, 7045 Trondheim, Norway
[b] HyBond AS, NAPIC, 7045 Trondheim, Norway

ARTICLE INFO

Associate Editor: Prof. M. Merklein

Keywords:
Additive manufacturing
Solid-state bonding
Aluminium alloys
HYB-AM

ABSTRACT

Hybrid Metal Extrusion and Bonding Additive Manufacturing (HYB-AM) is a new solid-state process for the production of 3D metal structures. In HYB-AM, the wire feedstock is continuously processed through an extruder and deposited in a stringer-by-stringer manner to form layers and eventually a near net-shape component. In this work, the layer bonding of AA6082 samples produced by this process has been investigated by means of tensile testing, hardness measurements and microscope analyses. Furthermore, a novel method for the fabrication of miniature tensile specimens for assessing the bond strength across the layers is presented and applied. The test results reveal that the ultimate tensile strength is approaching that of the substrate material of the same alloy, yet with a somewhat lower elongation prior to fracture. Microscope analyses show that the bonded interfaces are fully dense; however, the fracture surfaces reveal regions of kissing-bonds and lack of bonding. Still, these preliminary investigations indicate that the HYB-AM process, upon further optimization, has the potential of processing high quality aluminum alloy components.

1. Introduction

Over the past years, additive manufacturing (AM) of metals has received massive research interest following its gradual adoption by industry. The use of AM-technology enables new design freedom and opens for mass customization of near net-shape or net-shape parts at reduced energy consumption and with less material waste compared to traditional subtractive processes. A variety of AM processes exists, each with its individual characteristics when it comes to parameters like feedstock materials, part complexity, deposition rates, form of feedstock material (powder, wire, sheet), source of fusion (e.g. electron beam, laser, ultrasound) or state of fusion (solid-state, melted-state) (ASTM, 2015). The latter parameter – state of fusion – is of particular interest regarding processing of aluminium alloys.

In the melted-state category, the use of aluminium has been limited to a few alloys due to the resulting "as-cast" microstructure inherited from the melting involved. Only recently, Martin et al. (2017) have demonstrated that this problem can be overcome by the addition of nanoparticles acting as nucleation sites for new grains upon solidification of AA7075 and AA6061, resulting in material strengths comparable to those of wrought materials. Still, many melted-state processes suffer from reduced deposition rate due to limitations in the melt pool size. In addition, the contractions occurring during solidification and subsequent cooling can lead to a build-up of large residual stresses in the structure, hence, causing global deformations and distortions.

Solid-state processes, on the other hand, have no such limitations in deposition rates, as long as the processing temperature is kept below the melting range of the material. This makes solid-state processes attractive for manufacturing of larger components. Moreover, it enables the use of advanced aluminium alloys.

In the solid-state category, processes based on ultrasonic consolidation of sheets and foils can be found, as first demonstrated by White (2003). Lately, the ultrasound technique has also been used for joining of wire feedstock material (Deshpande and Hsu, 2018). Another solid-state process used for AM purposes is friction stir welding (FSW), which has been demonstrated for joining of stacked metal plates (Palanivel et al., 2015). Also, a modified FSW process, where the feedstock is added through a rotating stirring tool, has been developed by Aeroprobe (Schultz and Creehan, 2014). In addition, a process based on friction welding has been developed, where the material is deposited onto the substrate using a rotating consumable rod (Dilip et al., 2011).

In this work, the Hybrid Metal Extrusion & Bonding Additive Manufacturing (HYB-AM) process is presented in its current development stage, along with an investigation of the mechanical integrity of samples produced from AA6082. HYB-AM is a new solid-state process using metal feedstock wire to deposit material in a stringer-by-stringer

* Corresponding author.
E-mail address: jorgen.blindheim@ntnu.no (J. Blindheim).

https://doi.org/10.1016/j.jmatprotec.2020.116684
Received 22 June 2019; Received in revised form 12 February 2020; Accepted 16 March 2020
Available online 19 March 2020

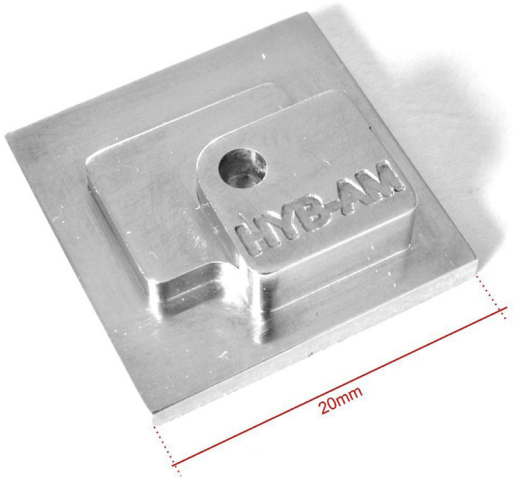

Fig. 1. A demo-part in aluminium produced by the HYB-AM process. Three layers are deposited onto a substrate plate, and subsequent subtractive machining is used to obtain the final net-shape.

manner to form layers and eventually a near net-shape structure. Subsequent to deposition, the part is finished by means of subtractive machining to achieve the desired net-shape, as depicted in Fig. 1. The potentials of this AM-process has previously been discussed by Blindheim et al. (2018, 2019a,b) and are further documented and explored in the present paper.

If a new manufacturing technology shall be attractive to industry, it needs to provide increased value compared to the currently available and proven manufacturing methods. A prerequisite, however, is that the mechanical integrity of the deposited material can compete with that of established production methods. In the case of HYB-AM, the bond strength between the individual stringers is considered to be the most critical quality requirement. Hence, a clarification of this point is the main objective of the presented study. Furthermore, to be able to subject the bonding interface to a pure tensile stress normal to the bonding interface it was necessary to develop a new tensile test technique as presented herein.

The following section provides an introduction to the working principles of the HYB-AM process, whereas Section 3 covers the experimental setup. Section 4 presents the results and discusses the outcome of the investigation in the light of the objective of this study. Finally, the conclusions are given in Section 5.

2. The HYB-AM process

The material flow in the HYB-AM process is based on the principle of continuous rotary extrusion, also known as Conform extrusion (Green, 1972). The extrusion step serves a dual purpose in this new AM process. First, the feedstock is heavily deformed in the extruder, which means that the oxides present on the feedstock surface become dispersed into the extrudate. Secondly, the extruder provides the required pressure to obtain bonding at the interface between the extrudate and the underlying structure. Following the illustration in Fig. 2a, the extrusion pressure is created by the frictional force between the feedstock wire and the tapered groove in the rotating wheel. The wheel is sealed by a stationary housing provided with an abutment and a die. The feedstock is firmly pressed into the groove and driven forward by the rotation of the wheel. Subsequently, the feedstock wire is blocked by the abutment and an axial compression is induced, causing the material to yield and fill the entire cross-section. This, in turn, increases the contact surface and friction, leading to further pressure build-up, ultimately causing the material to flow out of the die.

Fig. 2b illustrates the HYB-AM deposition sequence. The extruder adds material as it moves in the direction of deposition, placing stringers side-by-side to form a layer, thereby allowing new layers to be added on top of that. During deposition the die is continuously scraping the top of the underlying layer and the side wall of the adjacent stringer to remove the surface oxide. This creates the required conditions for bonding with the extrudate. Prior to deposition a strip of aluminium is fixed onto the heated bed to act as a substrate upon which the first layer of material is deposited. The aluminium strip becomes levelled during deposition of the first layer. Still, it should have a flatness less than 0.5 mm to reduce the amount of material accumulation during scraping and deposition. The accumulated material is considered waste and the scraping depth should therefore be minimized. Note that the metal flow and the bonding mechanisms in the HYB-AM process bear a close resemblance to those observed in longitudinal seam welds of porthole-die extrusions. In the latter case, the welds are formed under high pressure as the material streams merge after flowing around the die-bridges, as reviewed by Akeret (1992) and later by Valberg (2002). However, in HYB-AM, the merging metal streams should be considered as mating streams of extrudate and substrate, as illustrated in Fig. 3.

3. Experimental

3.1. Equipment

The individual components of the extruder were produced from hardened Uddeholm Orvar Supreme tool steel. The extruder is depicted in Fig. 4a. A Sieg SX3 CNC milling machine was used to control the speed and position of the extruder head. The rotation of the wheel is provided by a 1.8 kW servo motor connected to a gearbox with a gear reduction of 30. A PID-controller is used in combination with Nichrome heat-cartridges and a K-type thermocouple to control the temperature of the heated bed during deposition. The extruder housing is, by the same means, pre-heated to reduce the flow stress of the feedstock material during extrusion. The experimental setup is depicted in Fig. 4b and some key data for the extruder are listed in Table 1.

3.2. Materials and process parameters

Fig. 5 shows a two-layered structure deposited on a substrate material. The operational conditions are summarized in Table 2. The feedstock material was a Ø1.6 mm wire of the AA6082-T4 type, produced by HyBond AS. The wire was made from a DC cast billet, which was homogenized, hot extruded, shaved and cold drawn to the final diameter. Rolled plates of 4 mm AA6082-T6 were used as substrate material. The rolling direction of the plate is parallel to the deposition direction. Table 3 gives the chemical composition of the AA6082 feedstock and substrate materials.

Following deposition, the samples were removed from the hot machine bed and immediately quenched in water. The samples were naturally aged at room temperature for two weeks to reach the relatively stable T4 condition prior to mechanical testing.

3.3. Mechanical testing

To sample the bond strength between the individual layers, a novel method for producing miniature specimens for tensile testing has been developed and applied in this study. By using a 2 mm end mill, material was removed by milling such that cylindrical shaped pillars with a length constituting the height of two stringers were remaining in the deposited sample. Next, by using a single cutting thread mill, more material could be removed to end up with dog-bone shaped specimens like depicted in Fig. 6a and b. The number of tested specimens are shown in Table 4, while their locations are indicated in Fig. 7a. The reduced section of the specimens has a length and a diameter of 0.52 mm and Ø1.0 mm, respectively. The total length of each specimen is 1.8 mm and the diameter of the head is Ø1.9 mm. A specially designed split collar is used to grip the head of the specimens, at the same

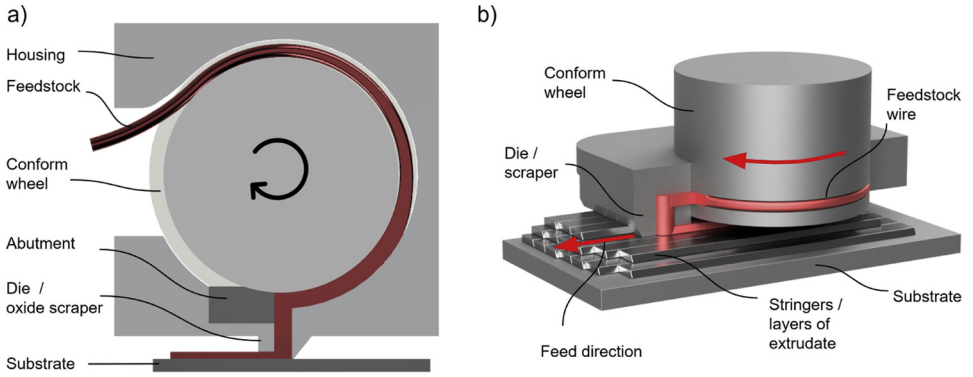

Fig. 2. Principal illustrations of the HYB-AM extruder; (a) The extruder consists of a wheel with a groove surrounded by a stationary housing. The feedstock wire is pressed into the groove, and upon rotation the extrusion pressure is built up as the material is blocked by an abutment close to the die. The die also acts as a scraper in order to remove oxides from the substrate prior to bonding with the extrudate; (b) Perspective view of the extruder and the deposited structure.

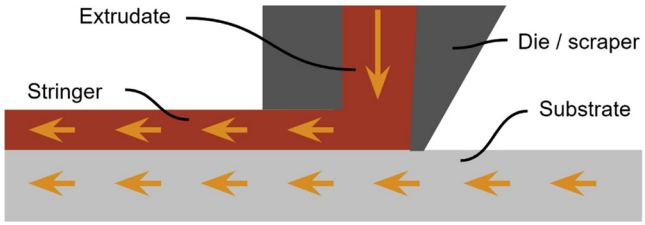

Fig. 3. In HYB-AM bonding is achieved as the metal streams of the oxide free extrudate and the scraped substrate merge at pressures exceeding the flow stress of the materials.

time as the sample is clamped to the lower part of the test machine, as shown in Fig. 6c. This method of producing miniature specimens allowed the bonded interface to be located in the region of the reduced section of the specimen while subjecting it to a pure tensile stress until fracture. The total displacement and the applied load are recorded by a MTS Criterion Model 42 ball screw universal testing machine employing a cross-head speed of 1 mm/min at a sampling frequency of 10 Hz.

Hardness measurements were made using a Mitutoyo Micro (HM200 series) Vickers hardness testing machine at a constant load of 1 kg. Six individual randomly located measurements were carried out on both the substrate and the extrudate for each sample section.

The samples used for microstructural analyses were prepared according to standard preparation procedures. To reveal the macrostructure, the samples were immersed in a water-based 1% sodium hydroxide solution for 4 min. The macrographs were captured using an Olympus BX35M light microscope and an Alicona Confocal Microscope. Finally, fracture surface analyses were carried out using a Quanta FEG 450 scanning electron microscope (SEM) at an acceleration voltage of 20 kV.

Table 1
Specifications for the HYB-AM extruder.

Parameter	Value
Wire diameter	1.6 mm
Maximum deposition rate	2150 g/h at 100 RPM
Outlet dimensions ($w \times h$)	4 mm × 1 mm
Extruder wheel outer diameter	28 mm

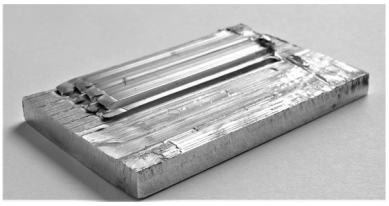

Fig. 5. Photograph of a two-layered sample of AA6082 (4 + 3 stringers).

Table 2
Parameters used in the present experimental setup.

Parameter	Value
Wheel rotation speed	4.0 RPM
Deposition feed rate	185 mm/min
Deposition rate	110 g/h
Wheel torque	220 Nm
Extruder pre-heating temperature	300 °C
Deposition temperature	500 °C

4. Results and discussion

The macrostructure of a transverse section of a sample is shown in Fig. 7. The interface between the substrate and the extrudate is clearly

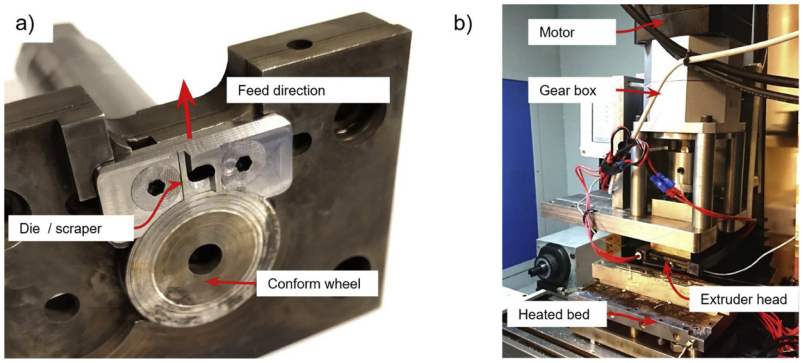

Fig. 4. Photographies of the experimental setup; (a) The current version of the HYB-AM extruder as seen from underneath; (b) The extruder assembly attached to the CNC machine.

Table 3
Chemical compositions (in wt%) of AA6082 feedstock wire (F) and substrate plate (S).

	Si	Mg	Cu	Fe	Mn	Cr	Zn	Ti	Zr	B	Others	Al
F	1.11	0.61	0.002	0.20	0.51	0.14	–	0.043	0.13	0.006	0.029	Balance
S	0.9	0.8	0.06	0.45	0.42	0.02	0.05	0.02	–	–	0.03	Balance

visible after leaching, showing that the mating interfaces have merged into a fully dense material. Still, the macrographs reveal some defects in the form of cracks, as depicted in Fig. 7c and d, indicating variable bonding quality. Two possible explanations for this crack formation can be put forward: (1) The contact pressure has been too low during deposition, prohibiting full metallic contact between the merging interfaces, or: (2) Oxide has re-formed on the interfaces due to oxygen exposure during deposition. The latter explanation is consistent with that observed in longitudinal seam welds in porthole die extrusion when a gas-pocket is present behind the bridge, as reported by Yu and Zhao (2018).

The mean tensile properties of all specimens are graphically presented in Fig. 8, showing that there is no significant difference in the ultimate tensile strength (UTS) of the layered material compared to the substrate material. Still, by considering the stress vs. displacement curve for one of the samples in Fig. 10, it is obvious that the elongation, and thus, the ductility is lower for the specimens extracted from the layer interface.

Fractographs of representative specimens (Fig. 9) also confirms this behaviour. Fig. 9a clearly shows regions with lack of bonding. Fig. 9b represents the specimen with the highest elongation prior to fracture, and even in this case, regions of kissing-bond formation are visible. Still, extensive dimple formation is observed, indicating that metallic bonding is obtained (Fig. 9d and e).

Fig. 9c shows a comparable fractograph of a specimen made from the substrate material. The dimple formation (f) is similar to that observed for the layer interface. The difference in cross-section is also noticeable, reflecting a more ductile response of the substrate specimens, as shown by the tensile test data in Fig. 10.

The results from the transverse hardness measurements are presented in Fig. 11. As can be seen from the figure, the hardness values are ~12% lower for the substrate material compared to the extruded material. The higher hardness of the extruded material is believed to be the result of the high silicon content of the extruded material, which contributes to significant solid solution hardening, as pointed out by Callister et al. (2013). In addition, the extrudate contains the dispersoid-forming elements Mn, Cr and Zr. These elements prevent recrystallization during deposition and therefore facilitate the formation of a substructure in the bonded layers with a high dislocation density and thus higher hardness than that of the substrate material (Hatch, 1984).

Table 4
Overview of test samples and number of tests conducted.

	Description	No.
Sample 1	Tensile specimens, substrate	3
	Tensile specimens, layer interface	4
	Vickers hardness, deposited material	6
	Vickers hardness, substrate	6
Sample 2	Tensile specimens, substrate	4
	Tensile specimens, layer interface	4
	Vickers hardness, deposited material	6
	Vickers hardness, substrate	6

5. Conclusions

Based on the results obtained in the study presented herein, the following conclusions can be drawn:

- The HYB-AM process can be used to deposit solid material of the AA6082 type in a stringer-by-stringer manner to form layers and eventually a near net-shape 3D-structure.
- During the extrusion process severe plastic deformation contributes to dispersion of the oxide being present on the surface of the feedstock into the extrudate. At the same time the HYB-AM extruder provides the required pressure to obtain bonding at the interface between the extrudate and the underlying structure.
- To assess the bond strength across the different layers a new method for fabrication of miniature tensile test specimens has been

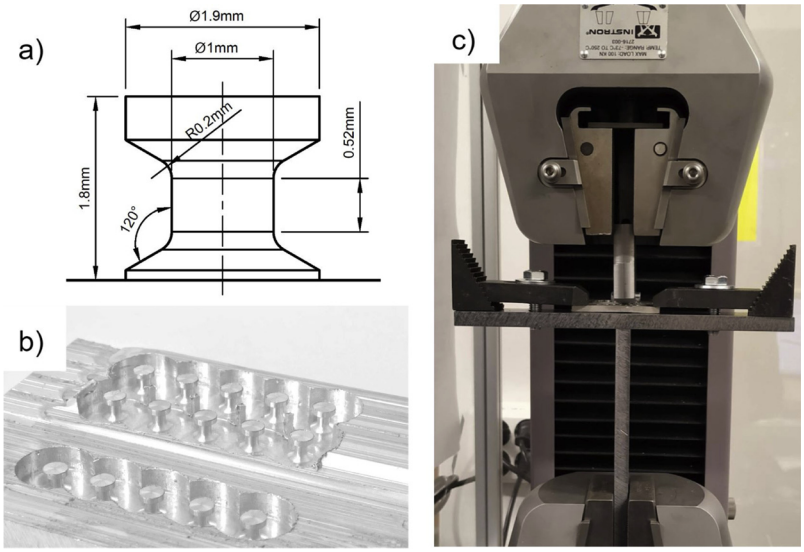

Fig. 6. The miniature tensile test technique developed and employed in the present study; (a) The geometry of a tensile specimen; (b) Photograph of specimens used for tensile testing of the substrate material and the layered structure; (c) Photograph of the tensile testing machine with a sample.

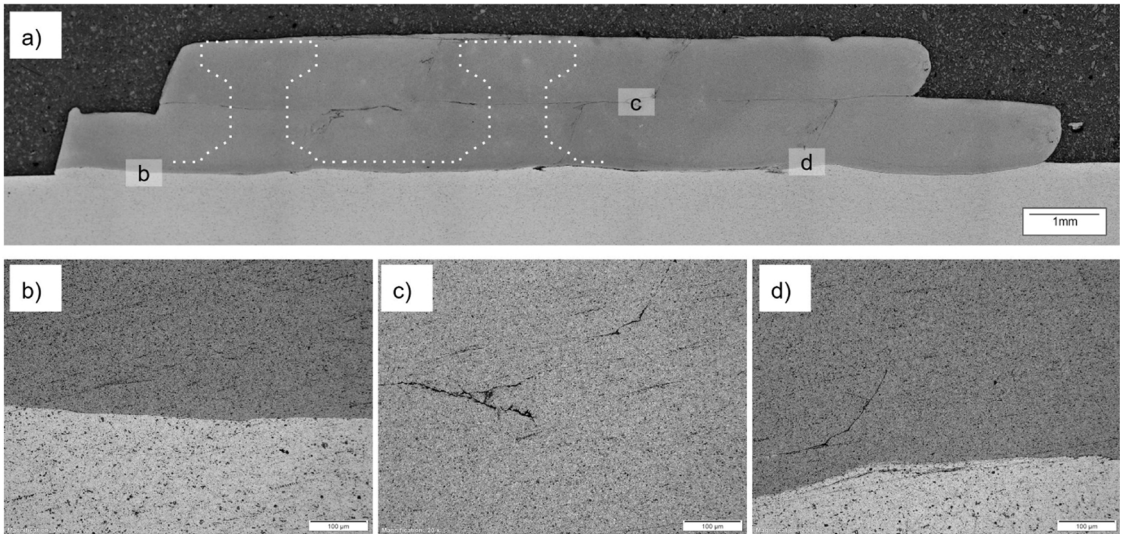

Fig. 7. Optical micrographs of; (a) Section of a deposited structure along with the superimposed contours of the tensile specimens; (b) The bonding interface between the substrate and the first layer; (c) and (d) Cracks observed at the interface between two stringers.

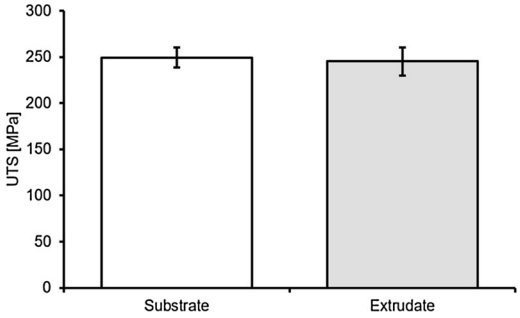

Fig. 8. Ultimate tensile strength of the substrate material ($n = 7$) and the bonded layers ($n = 8$). The error bars represent the standard deviation of the measurements.

developed. The specimens, which display a length equivalent to the height of two stringers, can be machined into the deposited sample and then tested in pure tension to reveal the full engineering stress-strain curve at different locations within the structure.

- The results from the mechanical testing show that the ultimate tensile strength of the bonded layers approaches that of the substrate material, yet with a lower elongation prior to fracture. Moreover, the subsequent fracture surface examination reveals evidence of extensive dimple formation, indicating that metallic bonding is achieved between the layers. Still, regions of kissing-bonds and lack of bonding are present, calling for further optimization of the HYB-AM process.

Author contributions

Conceived and designed the analysis: Jørgen Blindheim
Collected the data: Jørgen Blindheim
Contributed data or analysis tools: Jørgen Blindheim
Performed the analysis: Jørgen Blindheim, Øystein Grong
Wrote the paper: Jørgen Blindheim, Øystein Grong, Torgeir Welo, Martin Steinert
Other contribution: Torgeir Welo (Supervision), Martin Steinert

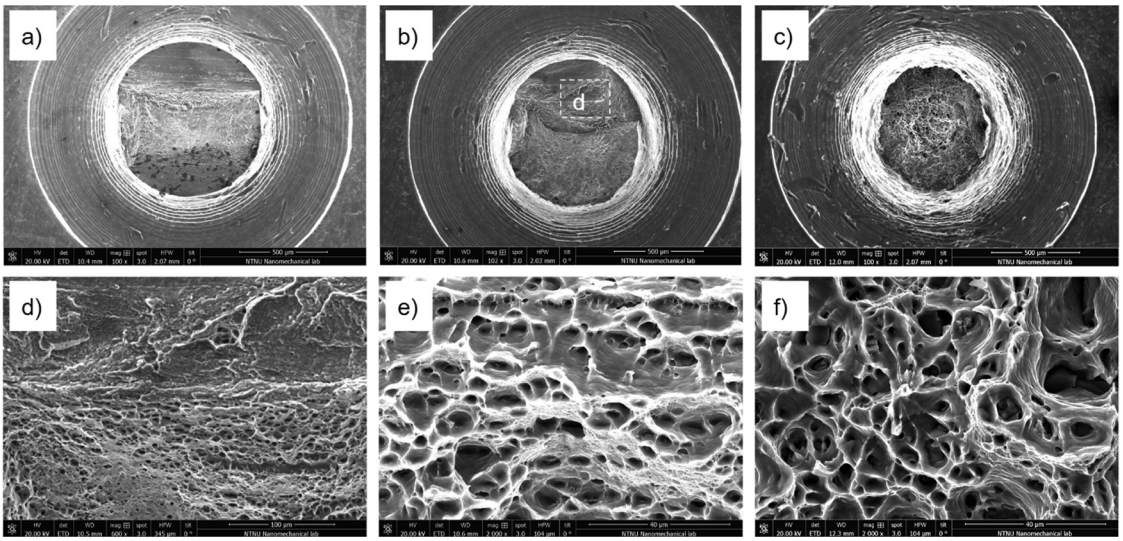

Fig. 9. SEM fractographs of fracture surfaces from three broken specimens. The corresponding tensile test results are plotted in Fig. 10; (a) Fracture surface of specimen B3; (b) Fracture surface of specimen B4; (c) Fracture surface of substrate specimen S1; (d) Mixed region with kissing-bond and dimple formation in specimen B4; (e) Dimpled fracture surface observed in specimen B3, and; (f) Dimpled fracture surface observed in specimen S3.

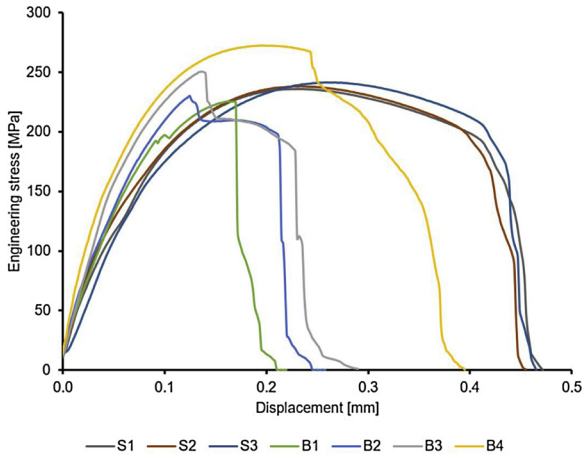

Fig. 10. Engineering stress vs. displacement curves for different tensile specimens. Included in the figure are four specimens, B1-B4, crossing two bonded layers, and three specimens representing the substrate material, S1–S3.

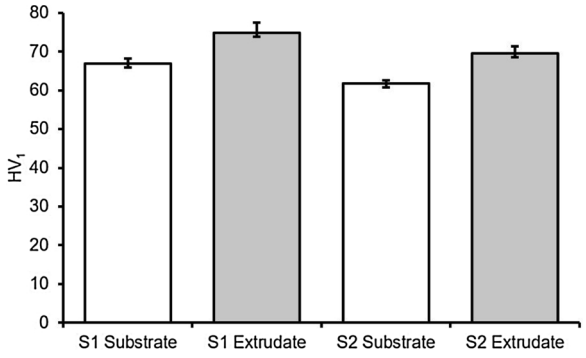

Fig. 11. Measured Vickers hardness of different samples.

(Project management and supervision)

Conflicts of interest

The authors declare no conflicts of interest.

Acknowledgements

The authors acknowledge the financial support from NTNU, NAPIC (NTNU Aluminium Product Innovation Center) and the KPN project Value sponsored by Research Council of Norway, Hydro and Alcoa.

References

Akeret, R., 1992. Extrusion welds-quality aspects are now center stage. Proceedings of the 5th International Aluminium Extrusion Technology Seminar 1992.

ASTM, 2015. Standard Terminology for Additive Manufacturing – General Principles – Terminology. ISO/ASTM 52900:2015(E).

Blindheim, J., Grong, O., Aakenes, U.R., Welo, T., Steinert, M., 2018. Hybrid Metal Extrusion & Bonding (HYB) – a new technology for solid-state additive manufacturing of aluminium components. Proc. Manuf. 26, 782–789. https://doi.org/10.1016/j.promfg.2018.07.092. https://linkinghub.elsevier.com/retrieve/pii/S2351978918307637.

Blindheim, J., Welo, T., Steinert, M., 2019a. First demonstration of a new additive manufacturing process based on metal extrusion and solid-state bonding. Int. J. Adv. Manuf. Technol. 9. https://doi.org/10.1007/s00170-019-04385-8.

Blindheim, J., Welo, T., Steinert, M., 2019b. Rapid prototyping and physical modelling in the development of a new additive manufacturing process for aluminium alloys. Proc. Manuf. https://doi.org/10.1016/j.promfg.2019.06.212.

Callister, W.D., Rethwisch, D.G., others, 2013. Materials Science and Engineering: an Introduction, ISBN: 978-1-118-47770-0, vol. 9.

Deshpande, A., Hsu, K., 2018. Acoustoplastic metal direct-write: towards solid aluminum 3d printing in ambient conditions. Addit. Manuf. 19, 73–80. https://doi.org/10.1016/j.addma.2017.11.006. https://linkinghub.elsevier.com/retrieve/pii/S2214860417300234.

Dilip, J.J.S., Rafi, H.K., Ram, G.J., 2011. A new additive manufacturing process based on friction deposition. Trans. Indian Inst. Metals 64, 27.

Green, D., 1972. Continuous extrusion-forming of wire sections. J. INST. MET. 100, 295–300.

Hatch, J., 1984. Aluminum: Properties and Physical Metallurgy. American Society for Metals, Materials Park (OH) ISBN: 978-0-87170-176-3.

Martin, J.H., Yahata, B.D., Hundley, J.M., Mayer, J.A., Schaedler, T.A., Pollock, T.M., 2017. 3d printing of high-strength aluminium alloys. Nature 549, 365–369. https://doi.org/10.1038/nature23894.

Palanivel, S., Nelaturu, P., Glass, B., Mishra, R., 2015. Friction stir additive manufacturing for high structural performance through microstructural control in an Mg based WE43 alloy. Mater. Des. (1980–2015) 65, 934–952. https://doi.org/10.1016/j.matdes.2014.09.082.

Schultz, J., Creehan, K., 2014. System for continuous feeding of filler material for friction stir welding, processing and fabrication, US Patent No. 8875976b2.

Valberg, H., 2002. Extrusion welding in aluminium extrusion. Int. J. Mater. Product Technol. 17, 497–556.

White, D.R., 2003. Ultrasonic consolidation of aluminum tooling. Adv. Mater. Process. 161, 64–65.

Yu, J., Zhao, G., 2018. Interfacial structure and bonding mechanism of weld seams during porthole die extrusion of aluminum alloy profiles. Mater. Charact. 138, 56–66. https://doi.org/10.1016/j.matchar.2018.01.052.